Isotopic evidence for partial geochemical decoupling between a Jurassic epicontinental sea and the open ocean

Silvia Danise [a,b,*], Gregory D. Price [a], Matthias Alberti [c], Steven M. Holland [d]

[a] School of Geography, Earth and Environmental Sciences, University of Plymouth, Drake Circus, Plymouth, Devon PL4 8AA, UK

[b] Dipartimento di Sicenze della Terra, Università degli Studi di Firenze, via La Pira 4, 50121 Firenze, Italy

[c] Institut für Geowissenschaften, Christian-Albrechts-Universität zu Kiel, Ludewig-Meyn-Straße 10, 24118 Kiel, Germany

[d] Department of Geology, University of Georgia, Athens, GA 30602-2501, USA

a b s t r a c t

We report stable isotope ratios ($\delta_{13}C$, $\delta_{18}O$),minor and trace elements (Mn, Fe, Sr,Mg) together with Ca concentrations from bivalve shells and belemnites from the Middle-Upper Jurassic Sundance Seaway (western United States), we compare them with coeval open-ocean Tethyan data, and reconstruct the palaeo-circulation of seawaywaters. The Sundance Seawaywas a 2000 kmlong epicontinental sea with a single entrance atmid latitudes (55–60°N), which would have fostered substantial evolution of seawater chemistry relative to its open-ocean source. Samples are distributed across the 13-million-year marine history of the seaway, and across a 540 km east-west transect spanningWyoming. Delta$_{13}$C values are in the same range as Tethyan data, and this suggests that they might record global changes in the carbon cycle, with one exception in the Oxfordian. Delta$_{18}$O values from the seaway are in contrast highly depleted compared with Tethyan data (−2 to −6‰), and they indicate unrealistically high palaeotemperatures (20–40 °C), assuming an isotopic composition of seawater of −1‰, as generally used for the Jurassic. Given more realistic temperature estimates from Mg/Ca ratios of bivalve shells (10–25 °C), we explain such negative $\delta_{18}O$ values by the southward inflow of normal-salinity, isotopically depleted (−3, −4‰), Arctic water into the seaway. Such water would become progressively more saline and denser as it flowed towards the southernmost portion of the seaway. In the Late Jurassic, characterised by wetter climate conditions, less dense Sundance waters may have instead exhibited a northward flow, reducing the southward surface flow from the Arctic. The observed partial geochemical decoupling of Sundance Seaway water masses from the open ocean strongly recommends caution in interpreting the geochemical record of ancient shallow seas, where local, regional and global drivers of change all need to be considered.

1. Introduction

The record of marine sedimentary rocks older than in situ oceanic crust is predominantly known from epicontinental deposits, which formed during periods of high relative sea level, in ancient epeiric seas (Holmden et al., 1998). As such, epeiric or epicontinental seaways are the dominant source for much of our information about ancient marine biodiversity. There is, however, growing evidence that these epeiric seaways are often decoupled from normal open-ocean conditions as a result of variations in water mass, depth, salinity, and stratification (e.g., Holmden et al., 1998; Brand et al., 2009; Petersen et al., 2016; Wierzbowski et al., 2018). Inland, semi-enclosed seas also tend to be more productive than the open ocean and more prone to anoxia (e.g., Diaz and Rosenberg, 2008). Hence, understanding these systems is critical to reconstruct the temporal changes and biogeographic patterns of marine biodiversity as well as the role epeiric seaways play in terms of ocean circulation, carbon cycling, and climate change. This research sets out to examine the Jurassic Sundance Seaway, an epicontinental sea that developed on the North American craton from the Bajocian to the Oxfordian (Fig. 1). The palaeogeography of the Sundance Seaway had a greatly elongated shape and is inferred to have had a single entrance located at a mid latitude, which was the only connection to the open ocean. Because of this, pronounced latitudinal temperature and salinity gradients have been suggested for the seaway (Stanley, 2010; McMullen et al., 2014; Danise and Holland, 2017), which would have in turn controlled patterns of faunal diversity, distribution, and immigration into the seaway. However, no detailed palaeoenvironmental reconstruction of the seaway based on geochemical proxies has been performed so far to test these hypotheses, and to better understand the connection of the seaway to the open ocean, previous studies having focused only on sparse oxygen stable isotope analyses of belemnite rostra (Bowen, 1961; Longinelli, 1969; Longinelli et al., 2002). To characterise the palaeoceanography and climatic setting of the Middle–Late Jurassic Sundance Seaway, a record of oxygen and carbon isotopes, Ca, minor and trace elements (Mn, Fe, Sr, Mg) is presented here from well-preserved bivalves (family Gryphaeidae) and belemnite rostra from the Twin Creek, Gypsum Spring and Sundance Formation (Fig. 2). This record covers the 13 million year marine history of the seaway and spans 540 km across the seaway from westernmost to eastern Wyoming (USA).
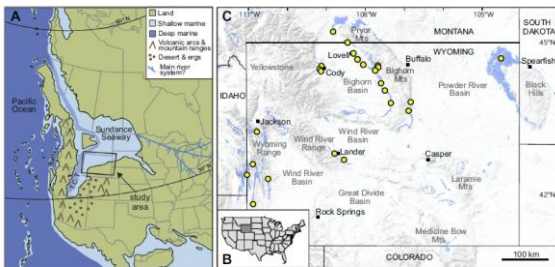

Fig. 1. Palaeogeographic reconstruction of western North America in the Middle Jurassic showing the Sundance Seaway and study area (A) and location map of the study area (B, C). A, modified from Blakey, 2014. Localization of desert, ergs and mountain ranges from Kocurek and Dott Jr. (1983); presence of a hypothetical transcontinental river from Dickinson and Gehrels (2003).

2. Geological setting

During the Middle–Late Jurassic (Bajocian to Oxfordian, ~170–157 Ma), the Sundance Seaway extended for nearly 2000 km from southern Utah northward into Alberta and British Columbia (Fig. 1; Imlay, 1957, 1980; Blakey, 2014). It was bounded to the west by a volcanic arc and a fold and thrust belt that separated it from the proto-Pacific Ocean, to the east by the North American craton, and to the south by the ancestral Rockies uplift that separated it from the Gulf of Mexico (Imlay, 1980). Most reconstructions of the seaway depict a single, narrow entrance at approximately 55–60°N palaeolatitude, with the seaway stretching southward through the Twin Creek Trough into Utah at ~30°N palaeolatitude (e.g., Blakey, 2014). The Sundance Seaway formed within a retroarc foreland basin, with the thrust loads to the west creating the deeper water Twin Creek Trough along the western margin, in which water depth was perhaps at most 100 m (Imlay, 1980; Kvale et al., 2001). The single entrance, length, and shallowness would likely have allowed for strong gradients in temperature and salinity to develop along the great length of the seaway (Tang and Bottjer, 1996; Stanley, 2010; McMullen et al., 2014; Danise and Holland, 2017).

Initial flooding spread southward from the northern proto-Pacific Ocean, reaching southeastern British Columbia during the Early Jurassic (Imlay, 1957). The seaway continued to extend southward, reaching Wyoming during the Early Bajocian, as evidenced by deposition of marine sediments (Imlay, 1957; Brenner and Peterson, 1994) in the Gypsum Spring Formation across most of Wyoming and the Twin Creek Formation in westernmost Wyoming and Idaho. Marine deposition continued

in this region throughout the Jurassic, until the Late Oxfordian (Brenner and Peterson, 1994; McMullen et al., 2014), and is recorded by the Sundance Formation across most of Wyoming and the Preuss and Stump Formations in westernmost parts of the basin. In the Late Oxfordian to Early Kimmeridgian, the seaway filled with terrigenous sediment supplied primarily from the south, as the coastal plain recorded by the Morrison Formation prograded northward (Brenner and Peterson, 1994; McMullen et al., 2014).

The Gypsum Spring Formation unconformably overlies the Triassic Chugwater Group in the Bighorn Basin in central Wyoming, the Triassic to Jurassic Nugget Sandstone to the west and south, and the Permian to Triassic Spearfish Formation to the east in the Black Hills (Imlay, 1952; Pipiringos and O'Sullivan, 1978). The Gypsum Spring Formation was deposited on a northwestward-dipping mixed evaporate–carbonate–siliciclastic ramp (Clement and Holland, 2016). Of the three informal members, only the middle member is fossiliferous. This middle member contains the ammonites Defonticeras and Stemmatoceras in western Wyoming (Imlay, 1952) and the ammonites Defonticeras, Parachondroceras and Sohlites in the western Bighorn Basin (Imlay, 1956; Callomon, 1982), and it is therefore regarded as belonging to the middle-upper part of the Bajocian stage (Imlay, 1980).

The overlying Sundance Formation is divided into seven members (Wright, 1973; McMullen et al., 2014; Danise and Holland, 2018), and these record alternations between relatively shallow-water carbonate and siliciclastic environments and relatively deeper-water mudstone environments. The Canyon Springs and lower Hulett members are dominated by carbonate rocks, deposited mainly in the shallow subtidal and on ooid shoals (McMullen et al., 2014). Eastward and southward, the lower Hulett passes into a siliciclastic desert system dominated by dryland rivers and desert dunes of the Lak Member (Danise and Holland, 2018). The Stockade Beaver Shale separates the Canyon Springs and Hulett, and it was deposited on a mixed carbonate–siliciclastic shelf, with offshore, carbonate mudstone facies to the west, and siliciclastic offshore and offshore transition facies to the east (Wright, 1973). Ammonite biostratigraphy indicates that the Canyon Springs Sandstone was deposited in the late Middle to early Late Bathonian, and the Stockade Beaver Shale was deposited in the Late Bathonian (Imlay, 1980). The lower Hulett Member is correlated with the Callovian Macrocephalites macrocephalus Zone (Imlay, 1982). The upper Hulett Member is a siliciclastic incised-valley fill capped by transgressive ooid shoal facies (Danise and Holland, 2018), and it lacks biostratigraphically useful fossils. The fossiliferous Redwater Shale Member was deposited on a wave-dominated siliciclastic shelf, and the lower part is correlated
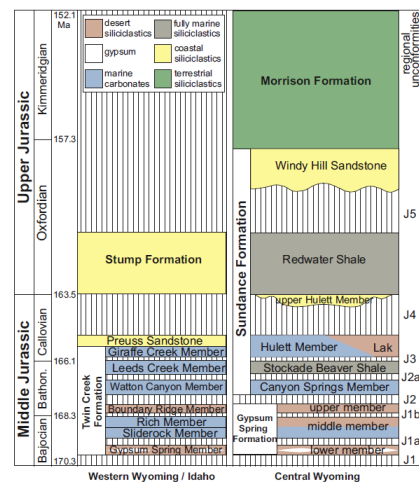

Fig. 2. Summary of the chronostratigraphic and sequence-stratigraphic framework of the Jurassic Twin Creek Formation in western Wyoming and Idaho and the Sundance Formation in central and eastern Wyoming. Chronostratigraphy of units is based on Pipiringos and O'Sullivan (1978), Imlay (1952, 1967, 1980), Brenner and Peterson (1994) and Kvale et al. (2001).

with the Oxfordian Cardioceras cordatum Zone (Imlay, 1982). The overlying Windy Hill Sandstone Member was deposited on a tidal coast and grades upward through progressive loss of tidal influence into overlying coastal plain deposits of the Morrison Formation (McMullen et al., 2014). Although the Windy Hill lacks biostratigraphically useful fossils, its stratigraphic relationship with the underlying Redwater Shale Member in southern Wyoming suggests that it is younger than Early Oxfordian and is probably Middle Oxfordian (Imlay, 1980). The Sundance Formation in Wyoming contains a rich assemblage of marine macroinvertebrates (Danise and Holland, 2017 and references therein), as well

as diverse but rare marine reptiles, including ichthyosaurs, plesiosaurs, and pliosaurs (McMullen et al., 2014; Massare et al., 2014).

Sediments of the Twin Creek Formation exposed in the Wyoming Range ofwesternmostWyoming and eastern Idaho consist of a thick series of marine carbonate and shale deposited on a westward-dipping mixed evaporate–carbonate ramp. The Twin Creek Formation is subdivided into seven members that were deposited in environments ranging from desert mudflat and sabkha to offshore carbonate (Imlay, 1967). Overlying the basal Gypsum Spring Member of the Twin Creek Formation, the Sliderock and Rich members contain the ammonites Stemmatoceras, Megasphaeroceras cf. M. rotundum, and Sohlites spinosus (Imlay, 1952, 1967, 1980),which belong to the middle-upper part of the Bajocian. The Leeds Creek Member has been biostratigraphically correlated to the Stockade Beaver Member of the Bighorn Basin, which indicates that the Giraffe Creek Member is also likely to be Late Bathonian to Callovian (Imlay, 1967). The Twin Creek Formation is overlain by theMiddle Callovian to Oxfordian Preuss and Stump formations, which were deposited in hypersaline intertidal mud flats (Kocurek and Dott Jr., 1983) and deltas.

In a recent sequence-stratigraphic interpretation of the marine Jurassic ofWyoming and adjacent states, the Twin Creek, Gypsum Spring and Sundance formations are divided into seven third-order depositional sequences, which include facies associations from offshore, carbonate ramp, siliciclastic wave-dominated shelf, siliciclastic tidal coast and mixed evaporate-siliciclastic desert depositional systems (McMullen et al., 2014; Clement and Holland, 2016; Danise and Holland, 2017, 2018). For this study, low-magnesium calcite shells of gryphaeid bivalves and belemnites were collected from every fossiliferous marine depositional sequence, and when possible, across the onshore–offshore gradient, which deepens towards the northwest.

3. Analytical methods

In this study,we integrate results fromgeochemistry of biogenic carbonate within a rigorous stratigraphic and sedimentologic framework to reconstruct palaeoenvironmental changes in the Sundance Seaway. Samples were collected from22 locationswithinWyoming, and 1 location in Montana, USA (Fig. 1). From each fossiliferous bed, bivalves

(Liostrea strigilecula, Gryphaea sp., G. planoconvexa, G. nebrascensis and Deltoideum sp.) and belemnites (Pachyteuthis densus) were collected for stable isotope and elemental analysis. 88 L. strigilecula, 5 Gryphaea sp., 28 G. planoconvexa, 53 G. nebrascensis, 59 Deltoideum sp., and 96 P. densus were analysed, for a total of 329 specimens. When possible, replicate analyses of the same shell for each species were performed to check the accuracy of the analyses, resulting in 371 analyses on 329 specimens (Supplementary Table S1).

The degree of diagenetic alteration of belemnite and bivalve shells was initially assessed on selected specimens through scanning electron microscope (SEM, Supplementary Fig. S1), cathodoluminescence (CL, Supplementary Fig. S2) and observations on thin sections, and then routinely performed on all specimens through minor and trace elements analysis (Supplementary Table S1). CL analyses were performed with a CITL MK5 cold cathodoluminescence instrument equipped with a Nikon microscope and digital camera, at the University of Plymouth, United Kingdom, on polished thin sections of shells cut longitudinally along the axis of maximum growth (perpendicular to the growth lines). CL iswidely employed as a screening technique to identify diagenetically

altered shellmaterial (e.g., Wierzbowski and Joachimski, 2007; Price and Teece, 2010; Alberti et al., 2012). The CL behaviour of marine carbonates is a good indicator of diagenetic alteration since many secondary calcites exhibit luminescence that is activated by Mn^{2+} which enters the calcite crystals after burial of the shell (e.g., Savard et al., 1995; Fürsich et al., 2005; Wierzbowski et al., 2009). As a result, nonluminescent

shells are generally considered to be unaltered (but see Barbin, 2013 for a critical review of themethod), compared with poorly preserved shells (showing the extensive presence of microborings, luminescent

microfractures and alteration associated with the apical area of belemnites). SEM observations, another excellent tool to detect post-depositional alteration of the shells (e.g., Korte and Hesselbo, 2011), were performed on the same thin sections, etched with 5% hydrochloric

acid for 2–3 s in order to reveal the detail of the microstructure, gold-coated with a Quorum Q150R ES, and studied with a ZEISS EVO MA15 at the University of Florence, Italy.

Amicrodrill and optical microscope were used to collect powder for stable isotopic and elemental analysis. Areas of the belemnite rostrum

and the outer and inner surface of bivalves typically most prone to diagenesis

and to the presence of possiblemicroborings and microfractures (e.g., Ullmann and Korte, 2015) were avoided. Between 0.3 and 0.5 mg were collected for each sample. Carbonate powders were reacted with 100% phosphoric acid at 90 °C. Evolved CO_2 was analysed on a GV Instruments Isoprimemass spectrometerwith a GilsonMultiflowcarbonate autosampler at the University of Plymouth. Results were calibrated against Vienna Pee Dee Belemnite (VPDB) using the international standard NBS-19 (National Bureau of Standards 19; $\delta_{13}C$ = 1.95‰ $\delta_{18}O$= −2.20‰). Reproducibility of replicate analyses for both $\delta_{18}O$ and $\delta_{13}C$ was better than 0.1‰. Each fossil shell was also sampled for Ca, minor and trace elements (Mn, Fe, Sr, Mg). Sample powders (between 3 and 10 mg) were reacted with 0.2 M HNO_3 and measured at the University of Plymouth using an Inductively Coupled Plasma-Atomic Emission Spectrometer (ICP-AES) using a PerkinElmer 3100. Repeat analyses of standards JLS-1 and BCS CRM393werewithin 2% of the certified values for Sr, Mn, Ca and Mg and 10% for Fe.
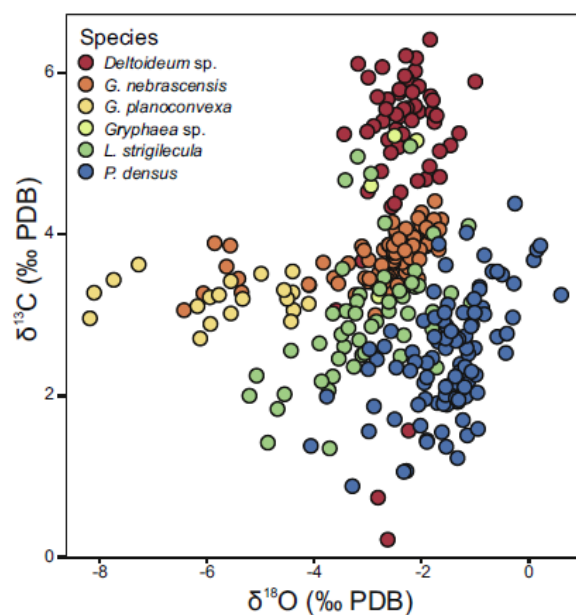

Fig. 3. Scatter plot of carbon isotopes versus oxygen isotopes of the studied fossil shells, with samples coded by species.

Four specimens of Gryphaea nebrascensis were selected for highresolution stable isotope analyses. The shells were cut parallel to the major growth direction, embedded in epoxy resin, and the cut surfaces were polished. Each specimen was examined under a cold CL microscope at the GeoZentrum Nordbayern of the Friedrich-Alexander-Universität Erlangen-Nürnberg, Germany. The shells of G. nebrascensis were largely non-luminescent and therefore considered to be wellpreserved; three specimens were selected for high-resolution stable isotope analyses. After identifying well-preserved sampling areas, the selected shells were sampled using a computer-controlled Merchantek Micromill (NewWave) at the GeoZentrum Nordbayern. Between 22 and 30 samples could be collected per shell from the inside (younger) to the outside (older) side of the shells with a resolution of about 3 to 4 samples per millimetre (Supplementary Fig. S3). The stable isotope composition was analysed using a carbonate preparation device (Kiel IV) connected to a ThermoScientific MAT 253 mass spectrometer at the Leibniz Laboratory for Radiometric Dating and Stable Isotope Research at the Christian-Albrechts-Universität zu Kiel, Germany. The carbonate samples were reacted within the preparation device with 100% orthophosphoric acid at 75 °C, and the evolved CO_2 gas was analysed using the mass spectrometer. Laboratory internal carbonate standards and two international carbonate standards (NBS-19 and IAEA-603) were analysed regularly to control the precision of measured $\delta_{13}C$ and $\delta_{18}O$ values. All values are reported in per mil relative to the Vienna Pee Dee Belemnite (VPDB) scale using NBS-19.

Palaeotemperature estimates were derived from the equation of Anderson and Arthur (1983)

assuming an ice-free Jurassic worldwith a $\delta_{18}O_{seawater}$ of−1‰V-SMOW (Shackleton and Kennett, 1975), and also fromMg/Ca (mmol/mol) ratio of bivalve shells, and calculated using the equation of Mouchi et al. (2013) calibrated on the modern Ostreidae Crassostrea gigas of the

northern eastern Atlantic Ocean:

$$T(°C) = 3.77 \cdot Mg/Ca + 1.88$$

where Mg/Ca is in mmol/mol.

Finally, carbon and oxygen stable isotopes of gryphaeids from this study were compared with Jurassic Tethyan oysters and belemnite isotope data derived from the literature (see Supplementary material for a complete list of the published referenced used).

Fig. 4. Record of carbon isotopes (A), oxygen isotopes (B), Mg/Ca temperatures (C), and δ¹⁸O$_{seawater}$ (D) plotted against the chronostratigraphic and sequence-stratigraphic framework of the Jurassic Twin Creek Formation and the Sundance Formation. Timescale of GTS 2012. Mg/Ca temperatures estimations for *P. densus* are not shown, as the applied equation is calibrated on modern oysters.
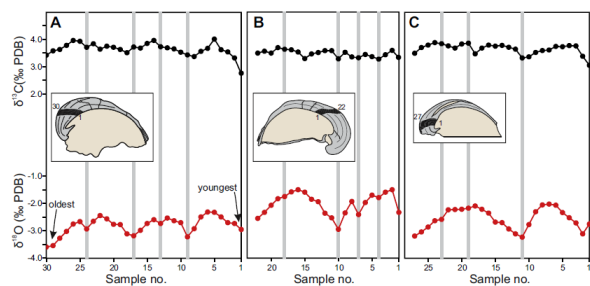
Fig. 5. High-resolution carbon and oxygen isotope record across three specimens of *Gryphaea nebrascensis*. Grey lines indicate dark bands on the shells which identify breaks in shell accretion (see Supplementary Fig. S3).

4. Results

4.1. Bivalve and belemnite preservation

Preliminary SEM observations on selected specimens indicated good textural preservation of the bivalve and belemnite samples. Observed specimens of G. nebrascensis and G. planoconvexa, belonging both to craton and foredeep settings, preserve the primary cross-foliated laminae of the inner layer (Supplementary Fig. S1). Good preservation is also supported by the low luminescence of most shell material, with the exceptions of some P. densus, in which the more porous apical canal is filled with luminescent, secondary calcite, and some gryphaeids, in which a few microborings or fractures are filled with micrite or sparry calcite (Supplementary Fig. S2). These areas tended to be Mn-rich as revealed bright orange luminescence (Supplementary Fig. S2), and they were either removed prior to, or avoided, during subsampling. Multiple studies have concluded that fossil ostreid and gryphaeid bivalves can be considered not diagenetically altered if they display Fe and Mn concentrations lower than 250 ppm, and Sr concentrations higher than 350 ppm (e.g., McArthur et al., 2000; Wierzbowski and Joachimski, 2007; Price and Page, 2008; Price and Teece, 2010; Schneider et al., 2009; Korte and Hesselbo, 2011). A total of 55 specimens were excluded from the dataset because their elemental concentration fell outside these values.

Similarly, several studies have shown that well-preserved belemnites typically have low concentrations of Mn (b100 ppm) and Fe (b250 ppm) and higher concentrations of Sr (c. 800–1600 ppm; e.g., Wierzbowski, 2002; Voigt et al., 2003; Price and Page, 2008; Wierzbowski et al., 2009; Price and Teece, 2010). All the investigated belemnites in this study had Fe concentrations below or equal to 250 ppm and Mn concentrations below 100 ppm (Supplementary Table S1). Only one specimen was excluded for having Sr concentration lower than 800 ppm.

Other evidences that the bivalves and belemnite shells are not diagenetically altered, aside from the low concentrations of Fe and Mn, are the low correlation between Fe and Mn concentrations and Sr/Ca ratios (Supplementary Fig. S4), and the scattered distribution of δ¹³C versus δ¹⁸O values for each species (Fig. 3; see also Ullmann and Korte, 2015). After microscopic and geochemical screening of the specimens, 312 of the initially prepared 371 samples were retained for subsequent data analyses and interpretation.

4.2. Carbon and oxygen isotopes through time and space

The variation in carbon and oxygen isotopic ratios (Figs. 3, 4, Supplementary Figs. S5, S6, Table S1) reflects the depositional environment and depositional sequence in which each species occurs in the Sundance. Most species in the Sundance Formation occur in only one depositional sequence and depositional environment, except Liostrea strigilecula which occurs in all the fossiliferous sequences of central Wyoming. In contrast, Gryphaea planoconvexa is limited to offshore facies of sequence J1a (Rich and Sliderock Member, Twin Creek Formation), which occurs only in the westernmost part of the studied area (Wyoming Range area, Figs. 1C, 4, Supplementary Fig. S6). Sequence J2 is only represented by samples of L. strigilecula collected from shallow subtidal facies in central Wyoming (Canyon Spring Member, Sundance Formation). Sequence J2a is mostly represented by G. nebrascensis, which occurs in offshore facies of central and western Wyoming (Cabin Creek Member of the Twin Creek Formation and Stockade Beaver Shale Member of the Sundance Formation), and by some L. strigilecula. Sequence J4 is very fossiliferous and contains specimens from L. strigilecula, Gryphaea sp., Deltoideum sp. and P. densus from offshore facies in central Wyoming (Redwater Shale Member, Sundance Formation). J5 is the only sequence from a tidal environment, and it contains fossils of L. strigilecula, Deltoideum sp., and P. densus from central Wyoming (Windy Hill Sandstone Member, Sundance Formation; Fig. 4, Supplementary Fig. S6). No data are present for sequence J3, as it is mostly characterised by terrestrial facies, coastal mudflat facies, and poorly fossiliferous oolitic carbonates (Kocurek and Dott Jr., 1983; McMullen et al., 2014), as such, the Callovian is not represented in our study. Because of the high turnover of species through time, and the differences in preserved depositional environments through time, it is difficult to discern well-defined temporal trends in carbon and oxygen stable isotope ratios (Fig. 4A, B). δ¹³C values for L. strigilecula, the only species which occurs in all sequences, albeit from different depositional settings, become progressively more positive from the Bajocian (median δ¹³C 2.5‰) to the Oxfordian (median δ¹³C 3.3‰). In the offshore facies association of sequence J4, the three different bivalve species display different mean values of δ¹³C, although their distributions partially overlap. Deltoideum sp. shows the most positive values of the three species (median δ¹³C 5.6‰), followed by Gryphaea sp. (median δ¹³C 4.9‰) and L. strigilecula (δ¹³C 4.0‰), and the belemnite P. densus has lower values (median 2.4‰) than bivalves.

Oxygen stable isotope values for Liostrea become slightly more positive from the Bajocian (median δ¹⁸O −3.7‰) to the Bathonian (median δ¹⁸O −2.7‰), and more negative again in the Oxfordian (median δ¹⁸O −3.3‰). In sequence J4, the three bivalve species show comparable values of δ¹⁸O, while samples from the belemnite P. densus are more positive (Fig. 3). Values of G. planoconvexa from the offshore facies association of sequence J1a of western Wyoming have the most negative δ¹⁸O values (median δ¹⁸O −5.6‰; min −8.1‰; Fig. 4A, Supplementary Fig. S6). The same very negative values only occur again in sequence J2a, in samples of G. nebrascensis from the offshore facies association of western Wyoming (Fig. 4B, Supplementary Fig. S6).

Focusing on L. strigilecula to compare the same species through time, the temperature trend obtained from δ¹⁸O values shows cooling from the Bajocian to the Bathonian, slight warming in the Late Bathonian, steady temperatures until the Early Oxfordian, and slight warming in the Middle–Late Oxfordian. All L. strigilecula samples come from an open-marine environment, except those of sequence J5 that come from a tidal siliciclastic coast, where salinity levels may have affected δ¹⁸O values. Assuming a δ¹⁸O$_{seawater}$ value of −1‰ V-SMOW, extremely high temperatures are implied by the δ¹⁸O values of samples of Gryphaea from western Wyoming of sequence J1a and J2a (up to 45–50 °C; Fig. 4B). Palaeotemperature estimates calculated using the equation of Mouchi et al. (2013) on bivalve shells Mg/Ca ratios, which applies a Mg/Ca-temperature calibration for the extant oyster Crassostrea gigas, show values around 10 °C lower than those obtained from oxygen stable isotopes (Fig. 4C, Supplementary Fig. S6). Other Mg/Ca temperature equations provide different absolute temperatures, as it is known that Mg/Ca calibrations are highly species-dependent (see Bougeois et al., 2016). For example, applying the equation of Lear et al. (2002) for low-Mg calcite (benthic foraminifera) to our fossil bivalve data results in temperatures that are slightly colder (by ~3–4 °C) than those derived using the equation of Mouchi et al. (2013) (Supplementary Table S1).

4.3. High-resolution carbon and oxygen isotopes on G. nebrascensis

High-resolution isotopic analysis was performed on three specimens of the thick-shelled gryphaeid G. nebrascensis, with 30, 22, and 27 isotopic measurements made on each (Fig. 5). Values of the carbon and oxygen
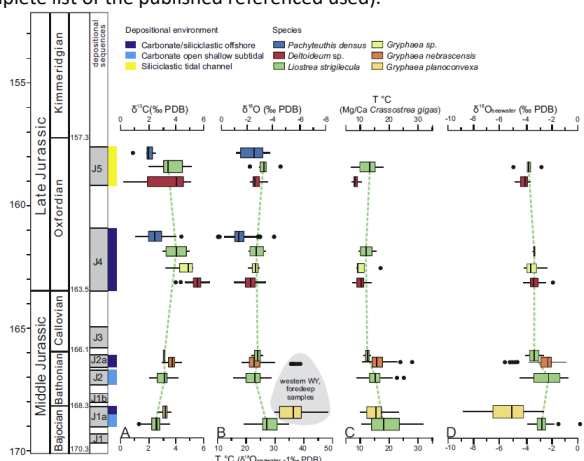
stable isotopic ratios are within those obtained from bulk sampling of the same species (Fig. 4A, B, Supplementary Fig. S6). $\delta_{13}C$ values range between 2.75 and 4.02‰ (average 3.60‰), and $\delta_{18}O$ range between −1.50 and −3.59‰ (average −2.50‰). The $\delta_{18}O$ of the three shells show a cyclical pattern. Three main cycles are clearly seen in the first shell, and 2 cycles in the remaining two. That the shown cyclicity is strictly connected with the growth of the shell, is confirmed by the evidence that the amplitude of the cycles decreases with ontogeny, as expected because younger shells have a higher growth rate (Ivany, 2012). More positive $\delta_{18}O$ values forma rounded, sinusoidal shape, while very negative values are truncated. The more negative peaks correspond to
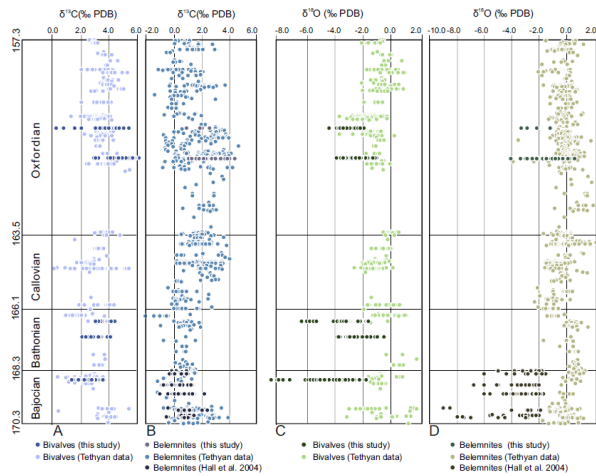

Fig. 6. Comparison of Sundance and Tethyan isotopes. A) Carbon isotopes of gryphaeid bivalves from this study compared with isotope data from Tethyan bivalves. B) Carbon isotopes of belemnite (*Pachyteuthis densus*) data from this study compared with isotope data from Tethyan belemnites and belemnites from the northern part of the Sundance Seaway (Fernie Formation) collected in British Columbia and Canada (Hall et al., 2004). C) Oxygen isotopes of gryphaeids from this study compared with isotope data from Tethyan bivalves. B) Oxygen isotopes of belemnite (*Pachyteuthis densus*) data from this study compared with isotope data from Tethyan belemnites and belemnites from the northern part of the Sundance Seaway (Fernie Formation) collected in British Columbia and Canada (Hall et al., 2004). See Supplementary material for a complete list of the published referenced used. Note that Tethyan isotope data include also data from the UK, a region where, throughout the Middle Jurassic, the fauna was characterised by both Tethyan influences from the south, and Boreal influences from the north (e.g., Korte et al., 2015). Numeric ages are from GTS 2012.

dark bands on the shell that are interpreted as periods of slowed shell growth (Jones and Quitmyer, 1996).

4.4. Comparison with Tethyan carbon and oxygen isotopes

Irrespective of sampling level, oxygen isotopic ratios from the gryphaeid bivalves in this study are consistently lighter than values reported from the Tethys, with little overlap in the data (Fig. 6C). In contrast, the carbon isotopic ratios coincide with Tethyan data, with the exception of those very positive $\delta_{13}C$ values derived largely from Deltoideum from sequence J4 (Oxfordian, Redwater Shale Member; Fig. 6A). Oxygen isotope data from the belemnites in this study are also consistently lighter than those reported fromTethys, againwith little overlap in the distributions (Fig. 6D). Similarly, carbon isotopic ratios in the belemnites fromthe Sundance Seaway coincidewith Tethyan carbon isotope data (Fig. 6B). The same pattern (light $\delta_{18}O$ data derived from the belemnites and $\delta_{13}C$ data that is similar to coeval Tethyan data) has also been observed in the Bajocian portion of the Fernie Formation of Alberta and British Columbia, Canada, deposited in the Sundance Seaway just to the north of the study area (Fig. 1; Hall et al., 2004).

5. Discussion

5.1. Isotopic composition of seawater and palaeotemperatures in the Sundance Seaway

The good preservation of our analysed low-Mg calcite bivalve and belemnite shells allow us to use their oxygen isotopic composition to infer the temperature and the oxygen isotope composition of ambient seawater when the shells formed. Compared with Tethyan oxygen isotope data, the oxygen isotope data derived from the Gryphaea, oysters and belemnites from the Jurassic Sundance Seaway are rather depleted in ^{18}O. Using an isotopic composition of seawater of−1‰(assuming an ice-free Jurassic world) and considering the full range of oxygen values (−0.5 to −8.6‰), the equation of Anderson and Arthur (1983) would indicate a temperature range of 10 to 50 °C (Fig. 4B). The upper range of these estimates is unrealistically high. Because screening of the shells with SEM, cathodoluminescence and trace elements argues against diagenetic effects, it suggests that the oxygen isotopic composition of seawater of the Sundance Seaway was substantially lighter than open ocean seawater. Using palaeotemperatures calculated from Mg/Ca ratios of bivalve shells and the equation of Anderson and Arthur (1983) to derive $\delta_{18}O_{seawater}$ suggests that the oxygen isotopic composition of seawater of the Sundance Seaway was much reduced (Fig. 4C, D). Continental runoff potentially provides a relatively light oxygen isotope source. Several studies (e.g., Wright, 1987; Petersen et al., 2016 for

the Cretaceous Western Interior Seaway) have documented relatively depleted $\delta_{18}O$ values from calcareous fossils and proposed that these suggest the influence of fresh water. A seaway with a $\delta_{18}O_{seawater}$ of −3.0 to−4.0‰would greatly decrease estimates of water temperature in the Sundance Seaway, putting them in line with the 10–26 °C temperature range derived from general circulation models of the Middle Jurassic for the region (e.g., Gugliotta et al., 2016), as well as palaeotemperatures derived from our Mg/Ca ratios of bivalves (Fig. 4C). The fully marine fauna of the Sundance Seaway (Imlay, 1957; McMullen et al., 2014; Danise and Holland, 2017) presents two challenges to invoking continental runoff. A seaway with a $\delta_{18}O$ value of−4.0‰would imply salinity substantially belownormal-marine conditions (~18–30 PSU). Second, the carbon isotopic composition of Sundance Seaway bivalves are similar to those of age-equivalent Tethyan calcitic bivalves, and both support positive fully marine values (Fig. 6A; see below). Furthermore, if reduced salinity was a significant factor, the greatest isotopic depletion would be expected in gryphaeids sampled from open shallow subtidal and tidal channel facies that are closer to land and freshwater influence. Instead, the lightest $\delta_{18}O$ values occur in Gryphaea fromthe offshore facies fromwesternmostWyoming (Fig. 4B, Supplementary Fig. S6). These offshore facies from westernmostWyoming
also have the greatest diversity in the Sundance Seaway (Danise and Holland, 2017), indicating that the light isotopic composition was not caused by freshwater input. Moreover, high runoff in the Middle Jurassicwould be unlikely, given the arid environment indicated by the extensive salinas, sabkhas, and wadi ephemeral rivers preserved in the J1a and J2 sequences (Danise and Holland, 2018). Although a fluvial system may have been present on the north-eastern borders of the seaway (see Dickinson and Gehrels, 2003) the direct impact of these freshwater influxes on salinity of this southern part is considered to be minor.
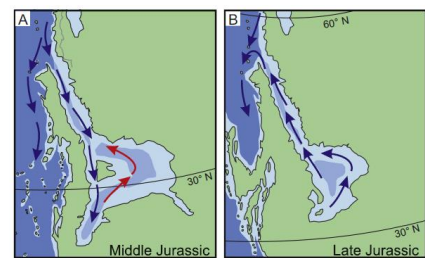

Fig. 7. Reconstruction of marine water circulation in the Sundance Seaway. A) Middle Jurassic, characterised by an arid climate system, with southward flow into the seaway (blue arrows) of isotopically light, surface marine waters from the Arctic region, and northward flow of more saline and denser (red arrows) Sundance Seaway waters. B) Late Jurassic, characterised by a semi-arid and winter–wet conditions, with a northward flow of less dense Sundance Seaway waters (blue arrows) that would inhibit the southward surface flow of ocean waters into the seaway.

In modern oceans, isotopically light seawater can also be observed in the Arctic Ocean (e.g., Bauch et al., 2015; Thomas and Mol, 2018). For example, the oxygen isotope composition of the modern Arctic Ocean, in the salinity range of 30–35 PSU (the Laptev Sea and the Mackenzie Shelf of the Beaufort Sea) can be as light as−4.5‰,with DIC carbon isotopic ratios being typically around 1.5‰, but in some cases exceeding 2.0‰. Similar isotopically light values for Arctic seawater have been hypothesised for the Cretaceous (Zhou et al., 2008), and these could reasonably
be extended to the Middle to Late Jurassic. Although Jurassic belemnite derived $\delta_{18}O$ values from Arctic and boreal domains are often more positive, ranging from 1.6 to −2.5‰ in the studies of Ditchfield (1997), Zakharov et al. (2005), Rogov and Price (2010), Zak et al. (2011) and Dzyuba et al. (2013), this does not preclude light $\delta_{18}O_{seawater}$ values, as temperatures were presumably a little cooler in these Arctic latitudes. The single entrance of the Sundance Seaway, located at a mid-latitude, would have been adjacent to a cool open shelf region occupied by a Boreal fauna that ranged southward from Alaska in cool waters sustained by the same southern Coriolis-driven current as today (Stanley, 2010). In contrast, the southern terminus of the seaway lay within the subtropical arid belt (Kocurek and Dott Jr., 1983; Kvale et al., 2001), where warm hypersaline conditions are supported by the occurrence of extensive evaporites and carbonate facies (Danise and Holland, 2018). If isotopically light seawater was derived from the Arctic, it would imply a southward flow into the seaway. North–south density differences and hence differences in hydrostatic level may have had an impact on water circulation. In the relatively arid Middle Jurassic, when Sundance Seaway water would have been more saline and therefore denser (creating a low hydrostatic sea level), surface water flow would have been southward, giving the water in the seaway Arctic characteristics, specifically light oxygen isotope ratios and typical marine DIC values (Fig. 7A). During the southerly transit along the length of the seaway, these normal-salinity waters would havewarmed and evaporation would have increased their salinity. This is supported by an increase in $\delta_{18}O$ of around 4‰of Middle Jurassic species from west to east within the seaway (Supplementary

Fig. S6, sequences J1a, J2, J2a), towards areas that are associatedwith extensive
desert mudflats, sabkhas, and wadi plain (Danise and Holland, 2018).

The temporal transition from Middle Jurassic carbonate-evaporite platform to a siliciclastic shelf towards the end of the Jurassic suggests regional climate change from subtropical arid conditions to temperate winter-wet conditions (Brenner, 1983), caused in part by the northward migration of the North American plate (Johnson, 1992). Increasingly temperate and wetter conditions may have increased freshwater runoff into the seaway. This fresheningwould have decreased seawater density in the seaway, reducing the net southward flow of water, possibly leading to net northward flow (Fig. 7B). The oxygen isotope data from bivalves of the Oxfordian Redwater Shale and Windy Hill Sandstone members show values that are closer to the Tethyan values (Fig. 6A). The $\delta_{18}O_{seawater}$ during this time was also likely to be close to typical Tethyan $\delta_{18}O_{seawater}$ values. An additional contributing factor to the resemblance between Tethyan and Sundance $\delta_{18}O$ values, may result from a wider opening of the Sundance Seaway during the Late Callovian – Early Oxfordian (Imlay, 1980) due to sea level highstand (Hallam, 2001;Wierzbowski et al., 2009), causing an increased connection to the open ocean.

Notwithstanding the isotopic decoupling between the Sundance Sea and the open ocean at the same mid-latitudes, and the resulting lowisotopic ratios, the temporal trends in palaeotemperature indicated by $\delta_{18}O$ of bivalves and belemnites and Mg/Ca ratios of bivalves, partially agree with those reconstructed for the Tethys. A Tethyan cooling event from the Bajocian to the Middle Bathonian has been inferred from the geochemistry of European bivalves and belemnites (Wierzbowski and Joachimski, 2007; Brigaud et al., 2008; Dera et al., 2011). The slight warming recorded in Europe in the latest Bathonian to the Early Callovian (Brigaud et al., 2008) is not observed in Sundance Mg/Ca data, but only in $\delta_{18}O$ values, and the concomitant change towards more negative isotope values of seawater (Fig. 4D), casts doubts on the validity of Sundance $\delta_{18}O$ values as a palaeothermometer in this instance. Both Sundance Mg/Ca and $\delta_{18}O$ record a slight warming from the Middle to the Late Oxfordian, which has been also recorded in Europe and in the Russian Platform (Brigaud et al., 2009; Dera et al., 2011; Wierzbowski et al., 2013).

5.2. Carbon cycle in the Sundance Seaway

The isotopic data presented here generally overlap those of the Tethys (Fig. 6), despite the potentially dynamic setting of the semienclosed Sundance Seaway. This suggests that the observed carbon isotope changes are not entirely decoupled from the open ocean (cf., Holmden et al., 1998).Moreover, these synchronous changes in $\delta_{13}C$ indicate global changes in the carbon cycle. Carbon cycling over timescales of millions of years results mainly from changes in the size and rate of the exchange between the Earth's surface carbon reservoirs and the lithosphere (e.g., Kump and Arthur, 1997), specifically the relative ratio of carbon stored in organic matter versus carbonates. For example, if relatively more carbon is removed from the oceans as organic matter that becomes buried, the $\delta_{13}C$ value of DIC in the ocean increases. If the observed $\delta_{13}C$ isotope data are linked tomarine carbon burial, continental margins and inland seas tend to be more productive than the open ocean (e.g., Diaz and Rosenberg, 2008) andmore prone to anoxia. This raises the question of whether the shallow Sundance Seaway was a significant locus of organic carbon burial. In the northern part of the Seaway, Lower Jurassic organic-richmudstone and limestone accumulated in west central Alberta and British Columbia (the Gordondale Member of the Fernie Formation), and these were deposited in a predominantly anoxic marine basin (Riediger and Bloch,

1995). These sediments contain up to 20 wt% TOC (Riediger and Bloch, 1995). Although,much of the Fernie Formation generally contains rocks with moderate to low concentrations of TOC (avg, 1.6 wt%), they are over mature, and their content is enough to be the source rock for several oil fields (Ryan and Morris, 2006).

In contrast, very positive $\delta_{13}C$ values (up to+6.4‰) found largely in Deltoideum from the Oxfordian Redwater Shale Member are much more positive than the Tethyan data (Fig. 6). Given that these values exceed those in the Tethys and are younger than the $\delta_{13}C$ excursion recognised in the Tethys during the Middle Oxfordian at the boundary between the plicatilis and transversarium ammonite zones (Głowniak and Wierzbowski, 2007), the most parsimonious interpretation of the data from the Sundance Seaway is that it reflects a regional carbon isotope excursion caused by burial of organic matter in the Sundance Seaway (e.g., Immenhauser et al., 2003). To date, no TOC data is available from the Redwater Shale Member. Higher $\delta_{13}C$ values, compared with Middle Jurassic records, are also observed in L. strigilecula and Gryphaea sp., even if less pronounced than in Deltoideum sp. Differences in $\delta_{13}C$

among these three species might be linked to species-specific vital effects (Immenhauser et al., 2016).

5.3. Seasonality in the Middle Jurassic

The growth of bivalve shells is strongly regulated by temperature and food availability (see Killam and Clapham, 2018), which vary periodically with tides, diurnal cycles, and seasons. Such variations are intimately related to the accretionary fabrics within the shells, which becomehigh-resolution biogeochemical recorders of the environmental and climatic conditions experienced during their lifetime (Schöne and Surge, 2012). The high-resolution isotope curves from G. nebrascensis of sequence J2a (Fig. 5) show cyclical patterns that we interpret as annual cycles, as observed in most fully marine bivalves (see Schöne and Surge, 2012), and the presence of these cycles argues that the isotopic composition of these shells has not be diagenetically reset. Minimum $\delta_{18}O$ values, which correspond to the warmest recorded water temperature, are associated with major darker bands on the shell (Fig. 5). This correspondence implies slower shell growth during the highest summer temperatures, as observed in modern bivalves (Killam and Clapham, 2018) and other species of fossil gryphaeids (Early Jurassic Gryphaea arcuata, Jones and Quitmyer, 1996). Peak temperatures probably coincided with periods of food limitation, which inhibited the growth of the shell, as supported by the correlation of many negative peaks in $\delta_{18}O$with low$\delta_{13}C$ values, probably linked to lower productivity. This implies that our G. nebrascensis shells provide a more complete record of the cooler portions of the year than thewarmer parts, suggesting that peak temperatures in the Sundance Seaway may have been somewhat higher than what is recorded in shells. This tendency for shells to reflect some portions of the year better than others, undetectable through bulk sample analysis, need to be considered when reconstructing past climates (see Ivany, 2012).

6. Conclusions

Carbon and oxygen stable isotope and elemental analyses on bivalve and belemnite shells from Middle–Upper Jurassic rocks of Wyoming allow for inferences on the climate, oceanography, and seasonality in the inland Sundance Seaway. These inferences are made possible by sampling within a rigorous sedimentologic and sequence-stratigraphic framework.

Oxygen isotopes are overall highly depleted (between −8.1 and 0.6‰) compared with coeval Tethyan data, suggesting that the Sundance Seaway was partly decoupled from the open ocean, and that the seawater within it had a light isotopic composition (between −3 and −4‰). The lowest isotopic ratios are observed in Middle Jurassic samples from the westernmost part of the basin deposited within the foredeep, and these decrease towards the east, where water depths were shallower. Given the fully marine conditions indicated by the diverse fauna, we hypothesise that the isotopically light seawater in the Middle Jurassic is best explained by the southward inflow of normalsalinity Arcticwaters into the seaway, characterised by light oxygen isotope values. This seawater would have become progressively more saline and denser as it flowed towards the southern end of the seaway, which occupied an arid setting in theMiddle Jurassic. In the Late Jurassic when the southern end of the seaway had a semi-arid winter-wet climate, increased freshwater run off would have made water in the Sundance Seaway less dense, reducing the southern flow and possibly leading to net northward flow of water.

Estimates of palaeotemperatures from Mg/Ca ratios of gryphaeid shells, indicates temperatures ranging from 10 to 26 °C, in agreement with temperature estimates fromglobal circulationmodels for theMiddle to Late Jurassic at the same palaeolatitudes. Carbon isotopic ratios from shells in the Sundance Seaway are closely similar to those from the Tethys, suggesting that observed synchronous changes in $\delta_{13}C$ reflect global changes in the carbon cycle through most of the Middle to Late Jurassic. The exception to this pattern is in the Early Oxfordian, where $\delta_{13}C$ ratios fromthe Sundance Seaway exceed those of the Tethys up to 2‰, which suggests a regional carbon isotope excursion caused by organic matter burial in the Sundance Seaway. Because epicontinental seas may have had reduced or limited exchange with the open ocean, it is important to consider that their geochemical history reflects regional processes as well as a global signal. Moreover, the results of this study imply caution when interpreting long-term trends in global climate and environmental change from large datasets.

References

Alberti, M., Fürsich, F.T., Pandey, D.K., 2012. The Oxfordian stable isotope record (δ_{18}O, δ_{13}C) of belemnites, brachiopods, and oysters from the Kachchh Basin (western India) and its potential for palaeoecologic, palaeoclimatic, and palaeogeographic reconstructions. Palaeogeogr. Palaeoclimatol. Palaeoecol. 344–345, 49–68.

Anderson, T.F., Arthur, M.A., 1983. Stable isotopes of oxygen and carbon and their application to sedimentological and paleoenvironmental problems. In: Arthur, M.A., Anderson, T.F., Kaplan, I.R., Veizer, J., Land, L. (Eds.), In Stable isotopes in sedimentary geology. SEPM Short Course. 10, pp. 1–151.

Barbin, V., 2013. Application of cathodoluminescence microscopy to recent and past biological materials: a decade of progress. Mineral. Petrol. 107, 353–362.

Bauch, D., Polyak, L., Ortiz, J.D., 2015. A baseline for the vertical distribution of the stable carbon isotopes of dissolved inorganic carbon (δ_{13}C DIC) in the Arctic Ocean. Arktos 1 (1), 15.

Blakey, R.C., 2014. Paleogeography and paleotectonics of the Western Interior Seaway. Jurassic–Cretaceous of North America. AAPG Search Discov. Artic. 30392.

Bougeois, L., De Rafélis, M., Reichart, G.J., de Nooijer, L.J., Dupont-Nivet, G., 2016. Mg/Ca in fossil oyster shells as palaeotemperature proxy, an example from the Palaeogene of Central Asia. Palaeogeogr. Palaeoclimatol. Palaeoecol. 441, 611–626.

Bowen, R., 1961. Paleotemperature analyses of Belemnoidea and Jurassic Paleoclimatology. J. Geol. 69, 309–320.

Brand, U., Tazawa, J., Sano, H., Azmy, K., Lee, X., 2009. Is mid–late Paleozoic ocean-water chemistry coupled with epeiric seawater isotope records? Geology 37, 823–826.

Brenner, R.L., 1983. Late Jurassic tectonic setting and paleogeography of western interior, North America. In: Reynolds, M.W., Dolly, E.D. (Eds.), Mesozoic Paleogeography of West-Central United States. Society of Economic Paleontologists and Mineralogists, Rocky Mountain Section, pp. 119–132.

Brenner, R.L., Peterson, J.A., 1994. Jurassic sedimentary history of the northern portion of the Western Interior Seaway, USA. In: Caputo, M.V., Peterson, J.A., Franczyk, K.J. (Eds.), Mesozoic Systems of the Rocky Mountain Region. USA. Society of Economic Paleontologists and Mineralogists, Rocky Mountain Section, Denver, Colorado, pp. 217–232.

Brigaud, B., Pucéat, E., Pellenard, P., Vincent, B., Joachimski, M.M., 2008. Climatic fluctuations and seasonality during the Late Jurassic (Oxfordian–Early Kimmeridgian) inferred from δ_{18}O of Paris Basin oyster shells. Earth Planet. Sci. Lett. 273, 58–67.

Brigaud, B., Durlet, C., Deconinck, J.-F., Vincent, B., Pucéat, E., Thierry, J., Trouiller, A., 2009. Facies and climate/environmental changes recorded on a carbonate ramp: a sedimentological and geochemical approach on Middle Jurassic carbonates (Paris Basin, France). Sediment. Geol. 222, 181–206.

Callomon, J.H., 1982. A review of the biostratigraphy of the post-lower Bajocian Jurassic ammonites of western and northern North America. In: Westermann, G.E.G. (Ed.), Jurassic–Cretaceous Biochronology and Paleogeography of North America. 27, pp. 143–174 Geological Association of Canada, Special Paper.

Clement, A., Holland, S.M., 2016. Sequence-stratigraphic context of extensive evaporites: Middle Jurassic Gypsum Spring Formation, Wyoming, U.S.A. Journal of Sedimentary Research 86, 965–981.

Danise, S., Holland, S.M., 2017. Faunal response to sea-level and climate change in a shortlived seaway: Jurassic of the Western Interior, U.S.A. Palaeontology 60, 213–232.

Danise, S., Holland, S.M., 2018. A Sequence stratigraphic framework for theMiddle to Late Jurassic of the Sundance Seaway,Wyoming: implications for correlation. basin evolution and climate change. Journal of Geology 126, 371–405.

Dera, G., Brigaud, B., Monna, F., Laffont, R., Pucéat, E., Deconinck, J.F., Pellenard, P., Joachimski, M.M., Durlet, C., 2011. Climatic ups and downs in a disturbed Jurassic world. Geology 39, 215–218.

Diaz, R.J., Rosenberg, R., 2008. Spreading dead zones and consequences formarine ecosystems. Science 321 (5891), 926–929.

Dickinson,W.R., Gehrels, G.E., 2003. U-Pb ages of detrital zircons from Permian and Jurassic eolian sandstones of the Colorado Plateau, USA: paleogeographic implications. Sediment. Geol. 163, 29–66.

Ditchfield, P.W., 1997. High northern palaeolatitude Jurassic-Cretaceous palaeotemperature variation: new data from Kong Karls Land, Svalbard. Palaeogeogr. Palaeoclimatol. Palaeoecol. 130, 163–175.

Dzyuba, O.S., Izokh, O.P., Shurygin, B.N., 2013. Carbon isotope excursions in Boreal Jurassic-Cretaceous boundary sections and their correlation potential. Palaeogeogr. Palaeoclimatol. Palaeoecol. 381–382, 33–46.

Fürsich, F.T., Singh, I.B., Joachimski, M., Krumm, S., Schlirf, M., Schlirf, S., 2005. Palaeoclimatic reconstructions of the Middle Jurassic of Kachchh (western India): an integrated approach based on palaeoecological, oxygen isotopic, and clay mineralogical data. Palaeogeogr. Palaeoclimatol. Palaeoecol. 217, 289–309.

Głowniak, E., andWierzbowski, H. 2007. Comment on "Themid-Oxfordian (Late Jurassic) positive carbon-isotope excursion recognised from fossil wood in the British Isles" by C.R. Pearce, S.P. Hesselbo, A.L. Coe, Palaeogeography, Palaeoclimatology, Palaeoecology 221, 343–357. Palaeogeography, Palaeoclimatology, Palaeoecology 248, 247–251.

Gugliotta, M., Fairman, J.G., Schultz, D.M., Flint, S.S., 2016. Sedimentological and paleoclimate modeling evidence for preservation of Jurassic annual cycles in sedimentation, western Gondwana. Earth Interact. 20 (19), 1–21.

Hall, R., McNicoll, V., Gröcke, D.R., Craig, J., Jonhston, K., 2004. Integrated Stratigraphy of the Lower and Middle Fernie Formation in Alberta and British Columbia, western Canada. Revista Italian di Paleontologia e Stratigrafia 110, 61–68.

Hallam, A., 2001. A review of the broad pattern of Jurassic sea-level changes and their possible causes in the light of current knowledge. Palaeogeogr. Palaeoclimatol. Palaeoecol. 167 (1-2), 23–37.

Holmden, C.E., Creaser, R.A., Muehlenbachs, K., Leslie, S.A., Bergström, S.M., 1998. Isotopic evidence for geochemical decoupling between ancient epeiric seas and bordering oceans: implications for secular curves. Geology 26, 567–570.

Imlay, R.W., 1952. Correlation of the Jurassic formations of North America, exclusive of Canada. Geol. Soc. Am. Bull. 63, 953–992.

Imlay, R.W., 1956. Marine Jurassic exposed in Bighorn Basin, PryorMountains, and northern Bighorn Mountains, Wyoming and Montana. Am. Assoc. Pet. Geol. Bull. 40, 562–599.

Imlay, R.W., 1957. Paleoecology of Jurassic seas in the western interior of the United States. Geological Society of America Memoir 67, 469–504.

Imlay, R.W., 1967. Twin Creek Limestone (Jurassic) in the western interior of the United States. U.S. Geological Survey Professional Paper 540, 1–105.

Imlay, R.W., 1980. Jurassic paleobiogeography of the conterminous United States in its continental setting. U.S. Geological Survey Professional Paper 1062, 1–134.

Imlay, R.W., 1982. Jurassic (Oxfordian and Late Callovian) ammonites from thewestern interior region of the United States. U.S. Geological Survey Professional Paper 1232, 1–102.

Immenhauser, A.M., Della Porta, G.P., Kenter, J.A.M., Bahamonde, J.R., 2003. An alternative model for positive shifts in shallow marine carbonate δ_{13}C and δ_{18}O. Sedimentology 50, 953–959.

Immenhauser, A., Schoene, B.R., Hoffmann, R., Niedermayr, A., 2016. Mollusc and brachiopod skeletal hard parts: intricate archives of their marine environment. Sedimentology 63, 1–59.

Ivany, L.C., 2012. Reconstructing paleoseasonality from accretionary skeletal carbonates: challenges and opportunities. In: Ivany, L., C., and Huber, B., T., (Eds.). Reconstructing Earth's Deep-time Climate. Paleontological Society Papers 18, 133–165.

Johnson, E.A., 1992. Depositional history of Jurassic rocks in the area of the Powder River Basin, northeasternWyoming and southeasternMontana. U.S. Geological Survey Bulletin 1917–J.

Jones, D.S., Quitmyer, I.R., 1996. Marking time with bivalve shells: oxygen isotopes and season of annual increment formation. Palaios 11, 340–346.

Killam, D.E., Clapham, M.E., 2018. Identifying the ticks of bivalve shell clocks: seasonal growth in relation to temperature and food supply. Palaios 33, 228–236.

Kocurek, G., Dott Jr., R.H., 1983. Jurassic paleogeography and paleoclimate of the central and southern Rocky Mountain Region. In: Reynolds, M.W., Dolly, E.D. (Eds.), Mesozoic Paleogeography of the West-central United States. SEPM Rocky Mountain Section, Denver, Colorado, pp. 101–116.

Korte, C., Hesselbo, S.P., 2011. Shallow marine carbon and oxygen isotope and elemental records indicate icehouse-greenhouse cycles during the Early Jurassic. Paleoceanography 26, PA4219. https://doi.org/10.1029/2011PA002160.

Korte, C., Hesselbo, S.P., Ullmann, C.V., Dietl, G., Ruhl,M., Schweigert, G., Thibault, N., 2015. Jurassic climate mode governed by ocean gateway. Nat. Commun. 6 10015.

Kump, L.R., and Arthur, M.A., 1997. Global chemical erosion during the Cenozoic: weatherability balances the budget. In: Ruddiman, W. (Ed.), Tectonics Uplift and Climate Change, Plenum Publishing Co., pp. 399–426.

Kvale, E.P., Johnson, G.D., Mickelson, D.L., Keller, K., Furer, L.C., Archer, A.W., 2001. Middle Jurassic (Bajocian and Bathonian) dinosaur megatracksites, Bighorn Basin, Wyoming, U.S.A. Palaios 16, 233–254.

Lear, C.H., Rosenthal, Y., Slowey,N., 2002. Benthic foraminiferalMg/Ca-paleothermometry: a revised core-top calibration. Geochim. Cosmochim. Acta 66, 3375–3387.

Longinelli, A., 1969. Oxygen-18 variations in belemnite guards. Earth Planet. Sci. Lett. 7, 209–212.

Longinelli, A., Iacumin, P., Ramigni, M., 2002. d_{18}O of carbonate, quartz and phosphate from belemnite guards: implications for isotopic record of old fossils and the isotopic composition of ancient seawater. Earth Planet. Sci. Lett. 203, 445–459.

Massare, J.A.,Wahl,W.R., Ross, M., Connely, M.V., 2014. Palaeoecology of the marine reptiles of the Redwater Shale Member of the Sundance Formation (Jurassic) of central Wyoming, USA. Geol. Mag. 151, 167–182.

McArthur, J.M., Donovan, D.T., Thirlwall, M.F., Fouke, B.W., Mattey, D., 2000. Strontium isotope profile of the early Toarcian (Jurassic) oceanic anoxic event, the duration of ammonite biozones, and belemnite palaeotemperatures. Earth Planet. Sci. Lett. 179, 269–285.

McMullen, S.K., Holland, S.M., O'Keefe, F.R., 2014. The occurrence of vertebrate and invertebrate fossils in a sequence-stratigraphic context: the Jurassic Sundance Formation, Bighorn Basin, Wyoming, U.S.A. Palaios 29, 277–294.

Mouchi, V., De Rafélis, M., Lartaud, F., Fialin,M., Verrecchia, E., 2013. Chemical labelling of oyster shells used for time-calibrated high-resolution Mg/Ca ratios: a tool for estimation of past seasonal temperature variations. Palaeogeogr. Palaeoclimatol. Palaeoecol. 373, 66–74.

Petersen, S.V., Tabor, C.R., Lohmann, K.C., Poulsen, C.J., Meyer, K.W., Carpenter, S.J., Erickson, J.M., Matsunaga, K.K., Smith, S.Y., Sheldon, N.D., 2016. Temperature and salinity of the Late Cretaceous Western Interior Seaway. Geology 44, 903–906.

Pipiringos, G.N., O'Sullivan, R., 1978. Principal unconformities in Triassic and Jurassic rocks, western interior United States: a preliminary survey. U.S. Geological Survey Professional Paper 1035–A.

Price, G.D., Page, K.N., 2008. A carbon and oxygen isotopic analysis of molluscan faunas from the Callovian–Oxfordian boundary at Redcliff Point, Weymouth, Dorset: implications for belemnite behaviour. Proc. Geol. Assoc. 119, 153–160.

Price, G.D., Teece, C., 2010. Reconstruction of Jurassic (Bathonian) palaeosalinity using stable isotopes and faunal associations. J. Geol. Soc. Lond. 167, 1199–1208.

Riediger, C., Bloch, J., 1995. Depositional and diagenetic controls on source-rock characteristics of the Lower Jurassic "Nordegg Member", western Canada. J. Sediment. Res. 65, 112–126.

Rogov, M.A., Price, G.D., 2010. New stratigraphic and isotope data on the Kimmeridgian–Volgian boundary beds of the Subpolar Urals, Western Siberia. Geological Quarterly 54 (1), 33–40.

Ryan, B., Morris, R., 2006. Gas Potential of the Fernie Shale, Crowsnest Coalfield, Southeast British Columbia. British Columbia Resource Development and Geoscience Branch, Summary of Activities, pp. 73–88.

Savard, M.M., Veizer, J., Hinton, R.W., 1995. Cathodoluminescence at low Fe and Mn concentrations: a SIMS study of zones in natural calcites. J. Sediment. Res. A65, 208–213.

Schneider, S., Fürsich, F.T., Werner, W., 2009. Sr-isotope of the Upper Jurassic of central Portugal (Lusitanian Basin) based on oyster shells. Int. J. Earth Sci. 98, 1949–1970.

Schöne, B.R., Surge, D., 2012. Bivalve sclerochronology and geochemistry. In: Seldon, P., Hardesty, J. (Eds.), Part N, Bivalvia, Revised, Volume 1. Treatise Online, Chapter: 14. Paleontological Institute Editors, p. 24.

Shackleton, N.J., and Kennett, J.P. 1975. Paleotemperature history of the Cenozoic and the

initiation of Antarctic glaciation: oxygen and carbon isotope analyses in DSDP sites
277, 279, and 289. Initial Reports of the Deep Sea 29, 743–755.

Stanley, S.M., 2010. Thermal barriers and the fate of perched faunas. Geology 38,
31–34.

Tang, C.M., Bottjer, D.J., 1996. Long-term faunal stasis without evolutionary coordination:
Jurassic benthic marine communities, Western Interior, United States. Geology 24,
815–818.

Thomas, H., and Mol, J. 2018. Dissolved inorganic carbon, total alkalinity, δ_{18}O-H$_2$O, δ_{13}CDIC,
temperature, and salinity collected from discrete bottle samples from CCGS
Amundsen in the Beaufort Sea during August and September 2014, PANGAEA,
https://doi.pangaea.de/10.1594/PANGAEA.886238, 2018.

Ullmann, C.V., Korte, C., 2015. Diagenetic alteration in low-Mg calcite frommacrofossils: a
review. Geological Quarterly 59, 3–20.

Voigt, S., Wilmsen, M., Mortimore, R.N., Voigt, T., 2003. Cenomanian palaeotemperatures
derived from the oxygen isotopic composition of brachiopods and belemnites:
evaluation of Cretaceous palaeotemperature proxies. Int. J. Earth Sci. 92,
285–299.

Wierzbowski, H., 2002. Detailed oxygen and carbon isotopic stratigraphy of the Oxfordian
in Central Poland. Int. J. Earth Sci. 91, 304–314.

Wierzbowski, H., Joachimski, M., 2007. Reconstruction of late Bajocian–Bathonian marine
palaeoenvironments using carbon and oxygen isotope ratios of calcareous fossils
from the Polish Jura Chain (central Poland). Palaeogeogr. Palaeoclimatol. Palaeoecol.
254, 523–540.

Wierzbowski, H., Dembicz, K., Praszkier, T., 2009. Oxygen and carbon isotope composition
of Callovian–Lower Oxfordian (Middle–Upper Jurassic) belemnite rostra from central
Poland: a record of a Late Callovian global sea-level rise? Palaeogeogr. Palaeoclimatol.
Palaeoecol. 283, 182–194.

Wierzbowski, H., Rogov, M.A., Matyja, B.A., Kiselev, D., Ippolitov, A., 2013. Middle–Upper
Jurassic (Upper Callovian–Lower Kimmeridgian) stable isotope and elemental records
of the Russian Platform: indices of oceanographic and climatic changes. Glob.
Planet. Chang. 107, 196–212.

Wierzbowski, H., Bajnai, D., Wacker, U., Rogov, M.A., Fiebig, J., Tesakova, E.M., 2018.
Clumped isotope record of salinity variations in the Subboreal Province at the
Middle-Late Jurassic transition. Glob. Planet. Chang. 167, 172–189.

Wright, R.P. 1973. Marine Jurassic ofWyoming and South Dakota: its paleoenvironments
and paleobiogeography. Museum of Paleontology, University of Michigan, Papers on
Paleontology 2, (49 pp.).

Wright, E.K., 1987. Stratification and paleocirculation of the Late Cretaceous Western Interior
Seaway of North America. Geol. Soc. Am. Bull. 99, 480–490.

Zak, K., Kostak, M., Man, O., Zakharov, V.A., Rogov, M.A., Pruner, P., Rohovec, J., Dzyuba,
O.S., Mazuch, M., 2011. Comparison of carbonate C and O stable isotope records
across the Jurassic/Cretaceous boundary in the Tethyan and Boreal Realms.
Palaeogeogr. Palaeoclimatol. Palaeoecol. 83–96.

Zakharov, V.A., Baudin, F., Dzyuba, O.S., Daux, V., Zverev, K.V., Renard, M., 2005. Isotopic
and faunal record of high paleotemperatures in the Kimmeridgian of subpolar
Urals. Russian Geology & Geophysics 46 (1), 3–20.

Zhou, J., Poulsen, C.J., Pollard, D., White, T.S., 2008. Simulation of modern and middle
Cretaceous marine δ_{18}O with an ocean-atmosphere